

---

# DISTRIBUTION RE-WEIGHTING AND VOTING PARADOXES

---

**Bijan Mazaheri\***

Eric and Wendy Schmidt Center  
Broad Institute of MIT and Harvard  
Cambridge, MA  
bmazaher@broadinstitute.org

**Siddharth Jain**

Department of Electrical Engineering  
California Institute of Technology  
Pasadena, CA  
sidjain@caltech.edu

**Matthew Cook**

Cortical Computation Group  
ETH Zürich  
Zürich, Switzerland  
cook@ini.ethz.ch

**Jehoshua Bruck**

Department of Electrical Engineering  
California Institute of Technology  
Pasadena, CA  
bruck@paradise.caltech.edu

## ABSTRACT

We explore a specific type of distribution shift called domain expertise, in which training is limited to a subset of all possible labels. This setting is common among specialized human experts, or specific focused studies. We show how the standard approach to distribution shift, which involves re-weighting data, can result in paradoxical disagreements among differing domain expertise. We also demonstrate how standard adjustments for causal inference lead to the same paradox. We prove that the characteristics of these paradoxes exactly mimic another set of paradoxes which arise among sets of voter preferences.

## 1 INTRODUCTION

The context of data can play an important role in the conclusions we draw from it. Two common examples of this are sampling bias and confounding effects, which have been addressed by advances in domain adaptation (Shimodaira, 2000; Sugiyama, Krauledat, and Müller, 2007; Sugiyama, Suzuki, et al., 2008) and causal inference (Pearl, 2009; Peters, Janzing, and Schölkopf, 2017) respectively.

Within domain adaptation, covariate shift refers to a difference between the training ( $p$ ) and target ( $q$ ) distributions of the non-label variables (called covariates), i.e.  $p(x) \neq q(x)$ . In the presence of covariate shift, minimizing a loss function on training data may over-emphasize regions where  $p(x)$  is large relative to  $q(x)$ , compromising accuracy for under-represented populations. A common technique for handling covariate shift involves weighting data according to the ratio of probabilities in the training and target distributions:  $w(x) = q(x)/p(x)$ . Such weighting ensures that training tasks minimize errors according to the target distribution  $q(x)$  instead of the training distribution  $p(x)$ .

This importance sampling approach crucially relies on the nature of the change in probability distribution, particularly that  $p(y | x) = q(y | x)$ . This assumption is often unrealistic: for example, a shift towards remote work during the pandemic drastically changed the relationship between commute time and household income (Mazaheri, Mastakouri, et al., 2023). Mazaheri, Mastakouri, et al., 2023 and Schölkopf et al., 2012 argue that this breakdown is governed by the causal structure of the system.

Causal structure can also be used to inform re-weighting techniques for estimating the effects of interventions. “Do-interventions” re-weight conditional probabilities according to marginal probability distributions on the covariates in order to dissociate relationships from confounding influence (Pearl, 2009)<sup>2</sup>. A similar approach involving weighting data according to the inverse of the probability of receiving a treatment, is referred to as “inverse propensity weighting” (Cole and Hernán, 2008; Hernán MA, 2020).

---

\*Work done during PhD at Caltech.

<sup>2</sup>Such techniques are sometimes referred to as a G-formula, or G-computation (Robins et al., 2009).

A common theme among these approaches is that re-weighting cannot be done blindly - instead we must carefully consider the system affecting our measured variables relative to the relationship we want to study. There has been little work investigating the effects of failing in this regard.

This paper will explore an often overlooked source of bias that we call **domain expertise**. In this setting, domain experts or ML models are capable of classifying *only a subset*  $\mathcal{Y}^* \subset \mathcal{Y}$  of the total possible classes for  $Y$ . An agent is fully aware of the relative probabilities of classes within this subset (i.e.  $\Pr(y_1^*)/\Pr(y_2^*)$  for  $y_1^*, y_2^* \in \mathcal{Y}^*$ ), but ignorant of any class outside of  $\mathcal{Y}^*$ . Agents therefore lack contextual information in the analysis of their data. For example, a “dogs vs. cats” classification task falls under domain expertise bias, but “dogs vs. non-dogs” does not. Such a setting is often common in the study disease propensities, where there the complement of those affected by the illness is not easily obtained.

The partial loss of labels within a domain expertise context shifts the distribution on the covariates. We will study a paradox that arises reweighting this shift either (1) according to standard covariate shift procedures or (2) when attempting to calculate interventional probabilities for causal inference. In the context of this paradox, domain experts form a cycle of preference on the most likely label or cyclically disagree on the causal effects of a treatment.

The paradox we will describe is very similar to the “Condorcet Paradox” from ranked choice voting, which has been studied for over 200 years (Nicolas et al., 1785). A single instance of this paradox, given by a graph with vertices representing candidates and edge-weights representing the “induced binary probabilities” will be referred to as a “linear ordering graph” (LOG). The analogous structure for the reweighted-data setting has been called an “expert graph” in Mazaheri, Jain, and Bruck, 2021. This paper will show that these two structures occupy the same space of weighted graphs (called the “linear ordering polytope”), meaning that results from ranked choice voting can be imported for characterizing networks of experts.

## 1.1 Summary

We will begin with in Section 2, which explores a few examples in more detail to understand how nontransitivity can emerge from covariate shift and inverse propensity re-weighting. We formalize this “expert graph” framework in Section 3, which closely follows Mazaheri, Jain, and Bruck, 2021 with some modifications to make the parallel to LOGs clearer. Section 4 then introduces linear ordering graphs (LOGs), which make up the “linear ordering polytope.” Section 5 proves that LOGs and expert graphs both occupy the linear ordering polytope. In Section 6, we conclude the paper and discuss the implications of the paradoxes we have introduced, and how we can use known results from the linear ordering polytope to aggregate opinions and knowledge.

## 1.2 Notation

In general, we will use the capital Latin alphabet (i.e.  $X, Y, T$ ) to denote random variables, with  $Y$  being the “label” or class we wish to predict or determine the causal effect on, and  $T$  being the a treatment. The lowercase Latin alphabet will denote assignments to these variables, i.e.  $x^{(1)}$  means  $X = x^{(1)}$ . Vectors and sets of random variables will be in bold-face font, while sets of assignments to random variables will use caligraphic font (i.e.  $\mathcal{Y} = \{y^{(1)}, y^{(2)}, \dots\}$ ). The following notation is used throughout the paper.

- $[\ell]$  is used to denote the set  $\{1, 2, \dots, \ell\}$  for any  $\ell \in \mathbb{N}$ .
- $\mathbb{1}[c]$  will be used for an indicator function which is 1 if condition  $c$  is met and 0 otherwise.
- $\mathbf{1}_\ell$  denotes an all 1 vector of size  $\ell$ .
- $\Delta^\ell$  will be used to denote vectors of length  $\ell$  which are probability distributions. That is,  $\lambda \in \Delta^\ell$  iff  $\lambda \in [0, 1]^\ell$  and  $\mathbf{1}^\top \lambda = 1$ .
- We use  $<, >, \leq, \geq$  to denote element-wise inequality. For example, we say  $\mathbf{w} \geq \mathbf{v}$  if  $w_i \geq v_i \forall i \in [\ell]$ .
- We will use  $\text{Co}(S)$  to denote the open convex hull of  $S$ ,  $\overline{\text{Co}}(S)$  to denote the closed convex hull, and  $\text{Bo}(\cdot)$  to denote the boundary.

## 2 EXAMPLES

We will illustrate our setting with a few hypothetical examples. Suppose we are given data that predicts whether a patient with a cough is suffering from a virus or cancer. Alternatively, we can imagine a human doctor who has primarily seen virus and cancer patients and is an expert at telling the difference between the two. Within this setting, suppose that a covariate  $X$  falls into three categories:  $x^{(1)}, x^{(2)}, x^{(3)}$ .

$X$	Cancer	Virus	Allergies
$x^{(1)}$	2	1	0
$x^{(2)}$	0	2	1
$x^{(3)}$	1	0	2

Table 1: A specification of counts for  $Y \in \{\text{Cancer, Virus, Allergies}\}$  and uniform distribution on  $X$ .

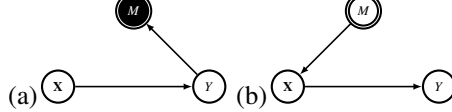


Figure 1: Two possible shifting models to explain a shift in distribution of  $X$ . (a) illustrates sampling bias on the label  $Y$ , which is the effect that we observe in domain experts. (b) illustrates a change in the distribution of  $X$  from a shift in an exogenous cause, or (equivalently) an intervention. We show that mistaking (a) for (b) gives nontransitive paradoxes.

## 2.1 Covariate Shift

One task is to estimate the prevalence of cancer within some population. From population surveys, we know that these categories of  $X$  are equally probable. However, the data that we observe has biased counts for  $x^{(1)}, x^{(2)}, x^{(3)}$  of 3, 2, 1. To correct for this bias we decide to weight each category by the inverse of its prevalence, such as weights of 2, 3, 6 ( $3 \times 2 = 2 \times 3 = 6 \times 1$ ).

For our three categories of  $X$ , we observe a respective prevalence of cancer of  $2/3, 0, 1$ . As our inverse weighting has made all three categories equally probable, we conclude that the prevalence of cancer is  $5/9$ . We call this conclusion the **situational opinion**, which is calculated as follows:

$$\frac{1}{3}(2/3 + 0 + 1) = 5/9. \quad (1)$$

**The Bigger Picture** The setting we have described is one which suffers from domain expertise bias because there is actually a third reason why patients may experience a cough: allergies. The full dataset is given in Table 1. Of course, limiting ourselves to the first two columns of this table massively biased our  $X$  distribution to the first two rows, as the third row is primarily populated by those who suffer from allergies.

**The Paradox** Now consider two separate studies done on the other two pairs of diseases. Perhaps a general practitioner only sees patients with allergies and viruses, and a housing-conditions inspector only sees cases of allergens and cancer. Each of these experts again decides to use re-weighting in order to bring all three values of  $X$  to parity. Notice that the numbers in Table 1 are intentionally the same, where each column is shifted down by one row from the column to its left. So, each expert makes the same calculation as in Equation 1. When these experts confer to share their results, they conclude that cancer is more prevalent than viruses, which is more prevalent than allergies, which is more prevalent than cancer.

**Resolution** The key issue lies in a misinterpretation of context. The correct causal model for our data bias is given in Figure 1 (a).  $M$  is an indicator function for membership of labels within an expert domain and hence the visible dataset is given by conditioning on  $M = 1$  data. The correct weighting (i.e. no re-weighting) would lead each expert to agree that the two diseases they studied were equally likely in the population (because the sum of every column in Table 1 is the same). However, re-weighting according to  $\Pr(X)$ , as implied by Figure 1 (b) yields the disagreement we have described.

## 2.2 Causality and Inverse Propensity Weighting

While the covariate shift example is the easiest to understand, similar paradoxes exist within causal inference as well. Suppose we wish to estimate the causal effect of treatment  $T$  on the prevalence of cancer  $Y$ . The principal difficulty in this task is the presence of some other covariate  $X$  which may confound our relationship between  $T$  and  $Y$  (see Figure 2 for a causal DAG of this setting).

Suppose that the entire distribution is given by Table 2, with marginally uniform distributions on  $T \in \{t^{(0)}, t^{(1)}\}$  and  $X \in \{x^{(1)}, x^{(2)}, x^{(3)}\}$ . These counts are chosen for illustration – while they do not directly imply the causal structure in

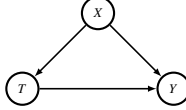


Figure 2: A DAG in which  $X$  confounds a treatment  $T$ 's effect on  $Y$ .

$T$	$X$	Cancer	Virus	Allergies
$t^{(1)}$	$x^{(1)}$	2	1	0
$t^{(1)}$	$x^{(2)}$	0	2	1
$t^{(1)}$	$x^{(3)}$	1	0	2
$t^{(0)}$	$x^{(1)}$	0	1	2
$t^{(0)}$	$x^{(2)}$	2	0	1
$t^{(0)}$	$x^{(3)}$	1	2	0

Table 2: A specification of counts for  $Y \in \{\text{Cancer, Virus, Allergies}\}$  for two treatments  $(t^{(0)}, t^{(1)})$  and three possible confounding states  $(x^{(0)}, x^{(1)}, x^{(2)})$ .

Figure 2, Appendix B shows how this can be remedied using perturbation on the counts that do not change the overall structure.

Now, again say we are restricted to the first two columns, i.e. cancer and virus patients. A do intervention is calculated using the backdoor criterion from Pearl, 2009,

$$\Pr(Y \mid \text{do}(t^{(1)})) = \sum_x \Pr(x) \Pr(Y \mid xt^{(1)}). \quad (2)$$

The do intervention differs from a conditional probability in that it marginalizes over the *marginal* probability distribution of  $X$  rather than one that is conditional on the treatment.

The numbers for the first three rows in Table 2 are the same as those in Table 1. The second set three rows are the additive complements, so that  $(Y, t^{(1)}, x^{(i)})$  and  $(Y, t^{(2)}, x^{(i)})$  always sum to the same count of 3. The result of this setup is that the marginal probability distribution is uniform, even in the domain-expertise setting. Consequently, we will observe the same cycle of preference when computing  $\Pr(Y \mid \text{do}(t^{(1)}))$  for the three domain experts, and the reverse cycle when computing  $\Pr(Y \mid \text{do}(t^{(0)}))$ .

The average treatment effect can be computed by taking the difference between the two do interventions, i.e.

$$ATE = \Pr(Y \mid \text{do}(t^{(1)})) - \Pr(Y \mid \text{do}(t^{(0)})). \quad (3)$$

As constructed, this yields an average treatment affect of  $5/9 - 4/9 = 1/9$ . That is, the cancer/virus expert believes that switching from treatment  $t^{(0)}$  to treatment  $t^{(1)}$  would prevent a virus in around  $1/9$  of the population, at the cost of increasing their risk of cancer.

As before, we can repeat these calculation for the two other experts, finding that switching from  $t^{(0)}$  to  $t^{(1)}$  decreases viruses relative to cancer, decreases allergies relative to viruses, and decreases cancer relative to allergies.

### 2.3 Inverse Propensity Weighting

Another technique for obtaining average treatment effects is inverse propensity weighting, which suggests that we weigh each datapoint  $(t, x, y)$  by  $1/\Pr(t \mid x)$  in order to create a pseudo-population in which  $T$  is independent from  $X$ . The average causal effect is the difference in expectations within this new pseudo-population (Hernán MA, 2020):

$$ATE = \mathbb{E}_{ps}[Y = \text{Cancer} \mid t^{(1)}] - \mathbb{E}_{ps}[Y = \text{Cancer} \mid t^{(0)}]. \quad (4)$$

This approach can be thought of as a re-weighting version of the backdoor criterion. Execution of this computation will show that the same numbers appear as with the backdoor criterion, resulting in equal weighting of each row and the same cycle of causal effects computed by the experts.

## 3 EXPERT GRAPHS

### 3.1 Formal Definition

We consider a prediction setting with:

State	$y^{(1)}$	$y^{(2)}$	$y^{(3)}$
$u^{(1)}$	.90	.09	.01
$u^{(2)}$	.01	.90	.09
$u^{(3)}$	.09	.01	.90

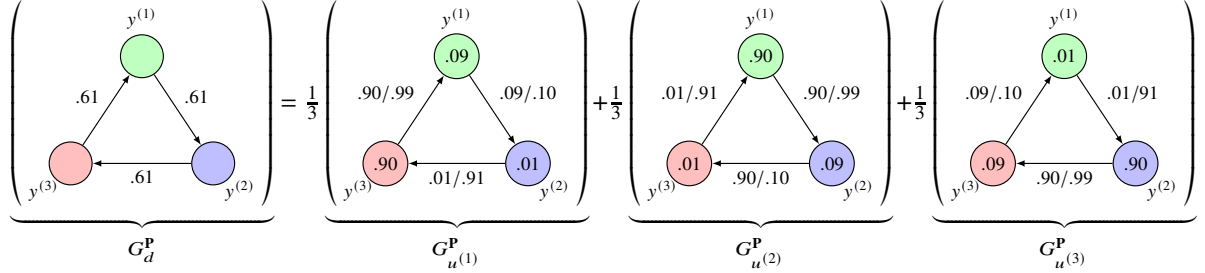


Figure 3: The expert graph  $G_d^P$  given by situational expert graphs with  $\mathbf{P}$  given in the table and  $d(\cdot)$  the uniform distribution. Probabilities from the table are given inside vertices of situational expert graphs, and expert opinions  $f_u(y^{(i)}, y^{(j)})$  are given as weights on edge  $y^{(i)} \rightarrow y^{(j)}$ . The expert graph  $G_d^P$  has edge-weights averaged over the situational expert graphs  $G_{u^{(1)}}^P, G_{u^{(2)}}^P, G_{u^{(3)}}^P$ .

- $U$ : Unknown value, but understood categorical distribution.
- $Y$ : Label of a classification problem.

This setting will contain two types of uncertainty. We represent uncertain input by a random variable  $U$  that takes values in alphabet  $\mathcal{U} = [k]$  with probability distribution  $d(\cdot) : \mathcal{U} \mapsto \Delta^k$ . Our label  $Y$  is a random variable partially determined by  $U$ . Specifically, each label  $Y$  will have a categorical distribution over alphabet  $\mathcal{Y} = \{y^{(1)}, y^{(2)}, \dots, y^{(n)}\}$  given unknown input  $u$ ,

$$p_u^{(i)} = \Pr(Y = y^{(i)} \mid u). \quad (5)$$

**Assumption 1.** We assume for any  $u \in \mathcal{U}$ ,  $\mathbf{p}_u > 0$ .

We refer to these  $n \times k$  probabilities as the “probability table,”  $\mathbf{P}$  (see Figure 3 for an example) and denote the vector of probabilities for a given input as  $\mathbf{p}_u \in \Delta^n$ .

We will study a graph whose vertices each represent an assignment to the label  $Y$ . The set of experts will be given by the edges,  $\mathcal{E} \subseteq \mathcal{Y} \times \mathcal{Y}$  each of which will encode a preference by a domain expert with an understanding of two label assignments.

**Definition 1.** Expert  $(y^{(i)}, y^{(j)}) \in \mathcal{E}$  has access to **situational opinions**  $f_u(y^{(i)}, y^{(j)})$  for each  $u \in \mathcal{U}$  given by the following conditional probability:

$$\begin{aligned} f_u(y^{(i)}, y^{(j)}) &:= \Pr(Y = y^{(i)} \mid Y \in \{y^{(i)}, y^{(j)}\}, u) \\ &= \frac{p_u^{(i)}}{p_u^{(i)} + p_u^{(j)}} \end{aligned} \quad (6)$$

**Observation 1.** From assumption 1,  $f_u(E) \in (0, 1) \forall e \in \mathcal{E}$ .

**Observation 2.**  $f_u(y^{(i)}, y^{(j)}) = 1 - f_u(y^{(j)}, y^{(i)})$ .

The union of many situational opinions gives a *situational expert graph*.

**Definition 2.** A **situational expert graph**  $G_u^P = (\mathcal{Y}, \mathcal{E}, f_u(\cdot))$  encodes experts’ pairwise situational opinions  $f_u(e)$  as weights on directed edges  $e = (y^{(i)}, y^{(j)}) \in \mathcal{E}$ .

We will study convex combinations of these situational expert graphs, which form aggregate opinions.

**Definition 3.** Expert  $e = (y^{(i)}, y^{(j)})$  will report their **aggregate opinion**, the expected value<sup>3</sup> of situational opinions:

$$\mathbb{E}_d[f_u(e)] = \sum_{u \in \mathcal{U}} d(u) f_u(e).$$

<sup>3</sup>In this paper we focus on discrete distributions for which the expectation is a sum. An extension to non-discrete distributions is naturally given by using an integral for the expectation.

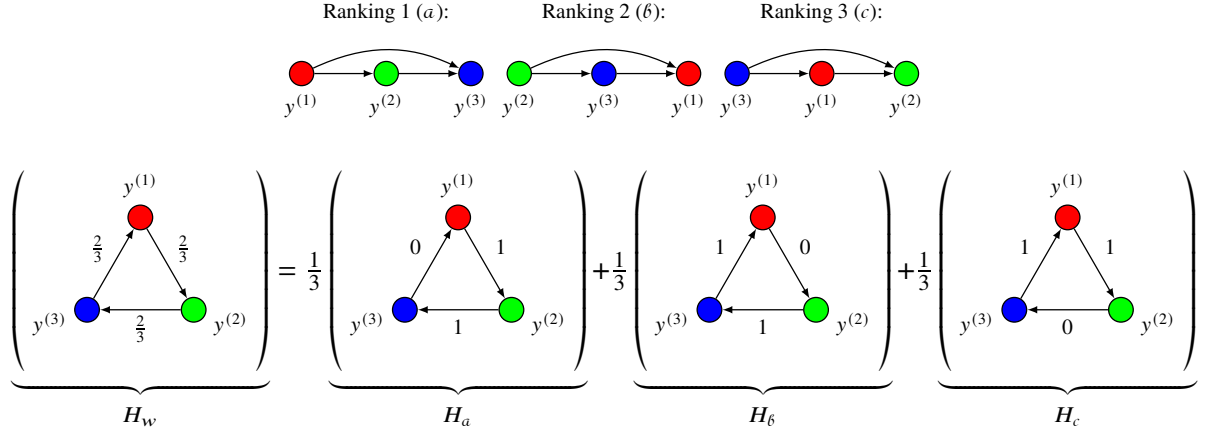


Figure 4: The LOG  $H_w$  given by ranking graphs from rankings  $a$ ,  $b$  and  $c$  and uniform  $w(a) = w(b) = w(c) = \frac{1}{3}$ . Edge-weights in  $H_w$  are averages over the edge-weights in  $H_a$ ,  $H_b$ ,  $H_c$  determined by the rankings. Decompositions of this form can be used to prove that  $H_w \in \text{Co}(\mathcal{H}_{\mathcal{R}}) = \mathcal{H}$ .

Expert graphs have edge-weights given by opinions marginalized over uncertainty in  $u$ .

**Definition 4.** An **expert graph**  $G_d^{\mathbf{P}} = (\mathcal{Y}, \mathcal{E}, f_d(\cdot))$  encodes experts' pairwise aggregate opinions  $f_d(e) = \mathbb{E}_d(f_u(e))$  as weights on directed edges  $e \in \mathcal{E}$ .

## 4 THE LINEAR ORDERING POLYTOPE

The “linear ordering polytope” is a well-studied class of weighted digraphs representing sets of possible pairwise elections in a population with ranked preferences of candidates (Fishburn, 1992). We will begin by formulating the linear ordering polytope as “Linear Ordering Graphs” (LOGs) which are convex combinations of “ranking graphs,” which is analogous to how expert graphs are formed from convex combinations of situational expert graphs.

**Definition 5.** A **ranking graph**  $H_{\tau} = (\mathcal{Y}, \mathcal{E}, f_{\tau}(\cdot))$  is a directed graph with given by an ordering  $\tau = (r_1, \dots, r_n)$  (where each  $r_i \in \mathcal{Y}$ ). The edge function  $f_{\tau}(\cdot) : \mathcal{E} \mapsto \{0, 1\}$  is given by the ordering,

$$f_{\tau}(r_i, r_j) = \mathbb{1}[i < j].$$

A *ranking graph* can be thought of as partial ordering of preferences given by a single voter. There are times when the structure of a graph is sparse enough to permit multiple possible rankings of vertices. Rankings graphs can also be thought of as *tournaments*, which are acyclic orientations given by 0, 1-weightings such that no cycle contains all the same edge-weight. Distributions over multiple ranking graphs/tournaments will give rise to net opinions described by LOGs.

**Definition 6.** A **linear ordering graph** (LOG)  $H_w = (\mathcal{Y}, \mathcal{E}, f_w(\cdot))$  encodes the probability of selecting a voter with a specific preference along each edge from a distribution on rankings (Fishburn, 1992)

$$f_w(y^{(i)}, y^{(j)}) = \mathbb{E}_w[f_{\tau}(y^{(i)}, y^{(j)})] = \sum_{r \in \mathcal{R}} w(r) f_r(y^{(i)}, y^{(j)}), \quad (7)$$

where  $\mathcal{R}$  has all  $n!$  possible orderings of indices.

An example of a LOG's decomposition into ranking graphs is given in Figure 4.

## 5 EQUIVALENCE BETWEEN EXPERT GRAPHS AND LOGS

As implied by our parallel formulation, expert graphs and LOGs make up the same space of weighted digraphs. We refer to the space of expert graphs as  $\mathcal{G}$ , the space of ranking graphs as  $\mathcal{H}_{\mathcal{R}}$ , then denoting the class of LOGs as the convex hull (excluding the boundary),  $\text{Co}(\mathcal{H}_{\mathcal{R}})$ .

**Theorem 1.** *The interior of the linear ordering polytope  $\text{Co}(\mathcal{H}_{\mathcal{R}})$  and the set of all possible expert graphs  $\mathcal{G}$  are equivalent. That is,  $G_d^{\mathbf{P}} = (\mathcal{Y}, \mathcal{E}, f_d(\cdot)) \in \mathcal{G}$  if and only if there exists  $H_w = (\mathcal{Y}, \mathcal{E}, f_w(\cdot)) \in \text{Co}(\mathcal{H}_{\mathcal{R}})$  with  $f_w(e) = f_d(e) \forall e \in \mathcal{E}$ .*

The next two subsections will focus on proving Theorem 1. In Subsection 5.1, we will give a reduction from any LOG to a probability table that generates an expert graph with the same pairwise edge weights. In Subsection 5.2, we will give a reduction from any expert graph to a set of rankings  $\tau \in \mathcal{R}$  and weights  $w(\cdot)$  that generate a LOG that matches the expert graph's pairwise weights. This equivalence will allow us to harness results from the linear ordering polytope framework to understand the power and limitations this paradox.

### 5.1 Reduction from LOGs to expert graphs

To show that any LOG can also be an expert graph, we will give a mapping from  $w(\cdot) : \mathcal{R} \mapsto [0, 1]$  to a set of states  $U$  with categorical distributions  $\mathbf{p}_u$  and probabilities  $\Pr(u) = d(u)$  such that  $f_d(\cdot) = \mathbb{E}_d[f_u(\cdot)]$  matches  $f_w(\cdot) = \mathbb{E}_w[f_\tau(\cdot)]$ .

We will first show how to give a set of class probabilities  $\mathbf{p}_u$  for which the pairwise expert output gets arbitrarily close to that of a ranking  $\tau$ . Here it will be convenient to think of the edge-weights as a vector  $\mathbf{f}_u = (f_u(e_1), \dots, f_u(e_m))$  and  $\mathbf{f}_d = (f_d(e_1), \dots, f_d(e_m))$ .

**Lemma 1.** *Let  $H_\tau = (\mathcal{Y}, \mathcal{E}, f_\tau(\cdot))$  be a ranking graph with  $\tau = (r_1, \dots, r_n)$ . For all  $\varepsilon > 0$ , we can construct a situational expert graph  $G_u^{\mathbf{P}} = (\mathcal{Y}, \mathcal{E}, f_u(\cdot))$  with a categorical distribution given by  $p_u^{(1)}, \dots, p_u^{(n)} \in (0, 1)$  such that*

$$\|\mathbf{f}_u - \mathbf{f}_\tau\|_2 = \sum_{e \in \mathcal{E}} (f_\tau(e) - f_u(e))^2 < \varepsilon. \quad (8)$$

*Proof.* Let  $t \in \mathbb{R}$ . Let  $\alpha_i = \frac{1}{t^i}$  and  $z = \sum_{i=1}^n \alpha_i$ . If we set  $p_u^{(r_i)} = \frac{\alpha_i}{z}$ , then

$$f_u^{(r)}(r_i, r_j) : \begin{cases} \leq \frac{1}{t} & \text{if } i > j \\ = \frac{1}{2} & \text{if } i = j \\ > 1 - \frac{1}{t} & \text{if } i < j \end{cases}.$$

Setting  $\frac{1}{t} = \frac{\varepsilon}{m}$  gives the desired result.  $\square$

We can use Lemma 1 to construct a state  $u_\tau$  with probability vector  $\mathbf{p}_u$  which achieves a  $f_{u_\tau}(\cdot)$  that is *very close* to  $f_\tau(\cdot)$  for each  $R \in \mathcal{R}$ .

The remainder of this reduction is given by showing the interior of the convex hull of our generated  $\mathbf{f}_u$  vectors is the same as the interior of the convex hull of  $\mathbf{f}_\tau$  vectors. To do this, we make use of the following more general result.

**Lemma 2.** *Consider a set of vectors  $\mathcal{V} = \{\mathbf{v}_1, \dots, \mathbf{v}_t\}$  and with  $\mathbf{v}_i \in \mathbb{R}^m$  for all  $i$ . If we have  $\tilde{\mathcal{V}}$  such that for every  $\varepsilon$  and  $\mathbf{v} \in \mathcal{V}$ , there exists  $\tilde{\mathbf{v}} \in \tilde{\mathcal{V}}$  such that  $\|\tilde{\mathbf{v}} - \mathbf{v}\|_2 < \varepsilon$ , then we have*

$$\text{Co}(\mathcal{V}) \subseteq \overline{\text{Co}}(\tilde{\mathcal{V}}). \quad (9)$$

The idea behind the proof of Lemma 2 will be to analyze the movement of the boundaries of the polytope defined by  $\mathcal{V} = \{\mathbf{v}_1, \dots, \mathbf{v}_m\}$  and corresponding polytope defined by the ‘‘perturbed points’’  $\tilde{\mathcal{V}} = \{\tilde{\mathbf{v}}_1, \dots, \tilde{\mathbf{v}}_m\}$ . The key is to show that a point that is far enough from the boundary of  $\text{Co}(\mathcal{V})$  will also be within  $\text{Co}(\tilde{\mathcal{V}})$ , given by Lemma 7. This required distance from the boundary will be relative to the amount by which the perturbed points have moved. As we bring the perturbation arbitrarily small (i.e.  $\varepsilon \rightarrow 0$ , all points in the interior of the polytope will be included. The full proof is given in the Appendix.

We are now able to conclude that the set of LOGs is contained in the set of expert graphs.

**Lemma 3.**  $\text{Co}(\mathcal{H}_{\mathcal{R}}) \subseteq \mathcal{G}$ .

*Proof.* Let  $\mathcal{G}_u$  be the space of *situational* expert graphs (i.e. not marginalized over  $U$ ). Lemma 1 shows that for every  $\varepsilon$  and  $H_\tau \in \mathcal{H}_{\mathcal{R}}$  there is some  $G_u^{\mathbf{P}} \in \mathcal{G}_u$  for which the edge-weight vectors are within  $\varepsilon$ :  $\|\mathbf{f}_u - \mathbf{f}_\tau\|_2 < \varepsilon$ . This satisfies the requirements for us to apply Lemma 2 by letting  $\mathcal{V} = \{\mathbf{f}_\tau : H_\tau \in \mathcal{H}_{\mathcal{R}}\}$  and  $\tilde{\mathcal{V}} = \{\mathbf{f}_u : (Y, \mathcal{E}, f_d(\cdot)) \in \mathcal{G}\}$  for Lemma 2. We conclude  $\text{Co}(\mathcal{H}_{\mathcal{R}}) \subseteq \overline{\text{Co}}(\mathcal{G}_u) \cong \mathcal{G}$ .  $\square$

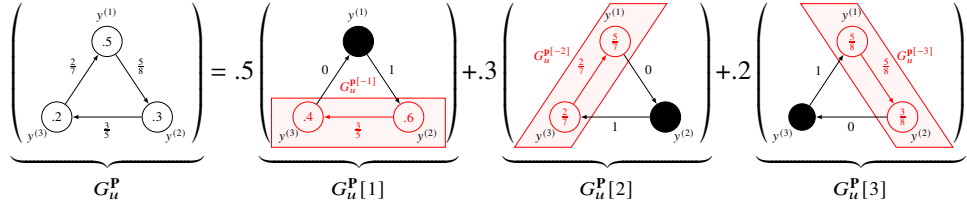


Figure 5: A decomposition of an expert graph  $G_u^P$  into prefix expert graphs  $G_u^P[1], G_u^P[2], G_u^P[3]$  following Lemma 4. Probabilities from probability table  $\mathbf{p}$  are shown inside the nodes in  $G_u^P$  and probabilities for  $\mathbf{p}[-i]$  are shown in red inside nodes in  $G_u^P[-i]$ . To get a decomposition into rankings  $H_r$  we apply the same procedure to the highlighted sub-graphs  $G_u^{P[-1]}, G_u^{P[-2]}, G_u^{P[-3]}$ . This determines the second choice distribution for each of these sub-populations, which will imply a third choice as well, giving a decomposition into rankings.

## 5.2 Reduction from expert graphs to LOGs

We will now show that, given an expert graph  $G_d^P = (\mathcal{C}, \mathcal{E}, f_d(\cdot))$ , we can find a decomposition into ranking graphs. The general approach will involve using the probability table of the expert graph to sort the population into sub-populations whose rankings have a constant ‘‘first choice’’ (Lemma 4). A recursion on each sub-population will then determine the distribution of second choices, and so on. A sketch of this procedure is given in Figure 5.

In order to describe the expert graph on the sub-population with a set of choices, we will use ‘‘prefix expert graphs.’’

**Definition 7.** Given an expert graph  $G_d^P = (\mathcal{Y}, \mathcal{E}, f_d(\cdot))$  and prefix  $a_1$  and non-specified leftover vertices  $\{b_1, \dots, b_{n-1}\}$ , we define the **prefix expert graph**  $G_d^P[a_1] = (\mathcal{Y}, \mathcal{E}, f_{G_d^P[a_1]}(\cdot))$  to be a graph with edge weights given by:

$$\begin{aligned} f_{G_d^P[a_1]}(a_1, b_j) &= 1, \\ f_{G_d^P[a_1]}(b_i, b_j) &= f_d(b_i, b_j). \end{aligned}$$

The prefix graph fixes  $a_1$  as the root of the tournament (or first choice in a ranking) while maintaining relationships between  $b_1, \dots, b_n$ .

**Lemma 4.** We can decompose any situational expert graph  $G_u^P = (\mathcal{Y}, \mathcal{E}, f_u(\cdot))$  with categorical distribution  $\mathbf{p}_u = (p_u^{(1)}, p_u^{(2)}, \dots, p_u^{(n)}) \in \Delta^n$  into prefix expert graphs with a distribution given by

$$G_u^P = \sum_i^n p_u^{(i)} G_u^P[a_1].$$

*Proof.* For this decomposition, the desired edge-weights  $f^*(e)$  for  $e = (y^{(i)}, y^{(j)})$  are achieved:

$$\begin{aligned} f^*(e) &= p_u^{(i)} \underbrace{f_{G_u^P[a_1]}(e)}_{=1} + p_u^{(j)} \underbrace{f_{G_u^P[a_1]}(e)}_{=0} + \sum_{a_1 \neq i, j} p_u^{(a_1)} \underbrace{f_{G_d^P[a_1]}(e)}_{=f_u(e)} \\ &= p_u^{(i)} + \sum_{a_1 \neq i, j} p_u^{(a_1)} f_u(e) \\ &= \left( p_u^{(i)} + p_u^{(j)} \right) \underbrace{\frac{p_u^{(i)}}{p_u^{(i)} + p_u^{(j)}}}_{f_u(e)} + \sum_{a_1 \neq i, j} p_u^{(a_1)} f_u(e) \\ &= \sum_{a_1=1}^n p_u^{(b_1)} f_u(e) = f_u(e) \end{aligned}$$

□

After Lemma 4 decides on the sub-population distribution for the ‘‘first choice,’’ we will recurse on each sub-population to determine the distribution on their ‘‘second choices.’’

**Definition 8.** We define  $G_u^{\mathbf{p}[-i]}$  to be the the subgraph of  $G_u^{\mathbf{p}}$  with  $y^{(i)}$  removed:

$$G_u^{\mathbf{p}[-i]} = (\mathcal{Y} \setminus \{y^{(i)}\}, E \setminus \{e : y^{(i)} \in e\}, f_u^{(-i)}(\cdot)).$$

**Observation 3.** The subgraph  $G_u^{\mathbf{p}[-i]}$  is generated by a new probability table with

$$p[-i]_u^{(j)} = \frac{p_u^{(j)}}{1 - p_u^{(i)}}. \quad (10)$$

**Lemma 5.** Given a situational expert graph  $G_u^{\mathbf{p}} = (\mathcal{Y}, \mathcal{E}, f_u(\cdot))$  with categorical distribution  $\mathbf{p}_u = (p_u^{(1)}, p_u^{(2)}, \dots, p_u^{(n)}) \in \Delta^n$ ,

$$w(r) = \prod_{i=1}^n \frac{p_u^{(r_i)}}{\prod_{j=1}^{i-1} (1 - p_u^{(r_j)})} = \frac{\prod_{i=1}^n p_u^{(r_i)}}{\prod_{i=0}^{n-1} (1 - p_u^{(r_i)})^{n-i}} \quad (11)$$

generates  $H_w = (\mathcal{Y}, \mathcal{E}, f_w(\cdot))$  with  $f_w(E) = f_u(E) \forall E \in \mathcal{E}$ .

*Proof.* Lemma 4 gives the decomposition

$$G_u^{\mathbf{p}} = \sum_{i=1}^n p_u^{(i)} G_u^{\mathbf{p}}[i].$$

Now, since the behavior of all edges  $\mathcal{E} \ni y^{(i)}$  is the same for all components in  $G_u^{\mathbf{p}}[i]$ , we can recurse on the sub-graph with  $y^{(i)}$  removed, with probabilities defined by Observation 3. The base case of  $\mathcal{Y} = \{y^{(j)}\}$  is trivial, with  $p_u^{(j)} = 1$ . Multiplication of the probabilities adjusted by Observation 3 gives Equation 11.  $\square$

Finally, we can give the desired result for this section.

**Lemma 6.**  $\mathcal{G} \subseteq \text{Co}(\mathcal{R})$ .

*Proof.* Pick  $G_d^{\mathbf{p}} \in \mathcal{G}$  without loss of generality. Decompose each state  $u$  using probability vector  $\mathbf{p}_u$  according to Lemma 5. Recall from Assumption 1 that all class probabilities  $p_u^{(i)} > 0$ , which yields  $w(r) > 0 \forall r \in \mathcal{R}$ . Hence,  $G_d^{\mathbf{p}} \subseteq \text{Co}(\mathcal{R})$ .  $\square$

## 6 DISCUSSION

### 6.1 A Warning

The main purpose of this paper is to introduce a new paradox that occurs when the context of domain expert bias is not properly considered. The paradox emerges when we consider multiple experts with differing, but overlapping domain biases.

This paradox serves as a warning to specific tasks in AI or ML with domain expert bias. While human subjects may be able to correct for the mistakes that lead to our paradoxes, the setting may be unavoidable in ML settings. Assigning relative probabilities to various cases (like asbestos vs. no asbestos) has an analogous setup in modern neural network architectures, which often include weighted sums of intermediary neurons. Of course, machine learning classifiers have no comprehension of context and no way of understanding the data that they have been given, nor do they have a strong understanding of the meaning of each of the neurons in their weighted sums. As a result, we must accept that cycles of preference are possible and likely when synthesizing model decisions at a higher level. Hence, studying this paradox in further depth will form a critical foundation under which we understand high-level decision fusion.

### 6.2 Special Properties of Expert Graphs

The combination of conclusions from multiple settings is sometimes referred to as decision fusion (Castanedo, 2013) or “network meta analysis” (Cipriani et al., 2013). Decision fusion is common in real world scenarios that involve studies on different pairs of treatments, or treatments vs. a placebo. This setting is also common among networks of AI or human agents for which we do not have a data-level understanding of decisions. In the presence of growing privacy concerns over the ever-expanding access to data, classifiers or AI models may precede direct access to the raw data that generated them, making the analysis of these networks even more essential.

In this paper, we showed that the space spanned by expert graphs is equivalent to the linear ordering polytope, which as many properties. For example, a cycle of opinions cannot be of arbitrary “strength.”  $A$  can be preferred to  $B$  and  $B$  to  $C$  and  $C$  to  $A$  with  $2/3$  frequencies, but not each with  $3/4$  frequencies. Mazaheri, Jain, and Bruck, 2021 called this the “curl condition,” which in general states that the sum of preferences along a cycle must not exceed one less than the length of that cycle (i.e.  $2/3, 2/3, 2/3$  is the limit to the non-transitivity for a cycle of length 3).

A convenient outcome of the limitations of the linear ordering polytope is that we can harness these limitations to provide bounds on “missing” experts, or edges without weights. That is, if we are missing a cancer/allergies expert, we can provide bounds on what opinion they will likely have. Furthermore, we can detect sources of error when these properties are violated. Hence, the equivalence between expert graphs and LOGs opens new doors for decision fusion and network meta analysis to help us synthesize ideas from many places.

## References

Castanedo, Federico (2013). “A review of data fusion techniques”. In: *The scientific world journal* 2013.

Cipriani, Andrea et al. (2013). “Conceptual and technical challenges in network meta-analysis”. In: *Annals of internal medicine* 159.2, pp. 130–137.

Cole, Stephen R and Miguel A Hernán (2008). “Constructing inverse probability weights for marginal structural models”. In: *American journal of epidemiology* 168.6, pp. 656–664.

Fishburn, Peter C (1992). “Induced binary probabilities and the linear ordering polytope: A status report”. In: *Mathematical Social Sciences* 23.1, pp. 67–80.

Grünbaum, Branko et al. (1967). *Convex polytopes*. Vol. 16. Springer.

Hernán MA, Robins JM (2020). *Causal Inference: What If*. Boca Raton: Chapman & Hall/CRC.

Mazaheri, Bijan, Siddharth Jain, and Jehoshua Bruck (2021). “Synthesizing New Expertise via Collaboration”. In: *2021 IEEE International Symposium on Information Theory (ISIT)*, pp. 2447–2452. doi: [10.1109/ISIT45174.2021.9517822](https://doi.org/10.1109/ISIT45174.2021.9517822).

Mazaheri, Bijan, Atalanti Mastakouri, et al. (July 2023). “Causal information splitting: Engineering proxy features for robustness to distribution shifts”. In: *Proceedings of the Thirty-Ninth Conference on Uncertainty in Artificial Intelligence*. Ed. by Robin J. Evans and Ilya Shpitser. Vol. 216. Proceedings of Machine Learning Research. PMLR, pp. 1401–1411. URL: <https://proceedings.mlr.press/v216/mazaheri23a.html>.

Nicolas, Jean Antoine et al. (1785). *Essai sur l'application de l'analyse à la probabilité des decisions rendues à la pluralité des voix. Par m. le marquis de Condorcet,...* de l’Imprimerie Royale.

Pearl, Judea (2009). *Causality*. Cambridge university press.

Peters, Jonas, Dominik Janzing, and Bernhard Schölkopf (2017). *Elements of causal inference: foundations and learning algorithms*. The MIT Press.

Robins, JM et al. (2009). “Longitudinal data analysis”. In: *Handbooks of modern statistical methods*, pp. 553–599.

Schölkopf, Bernhard et al. (2012). “On causal and anticausal learning”. In: *arXiv preprint arXiv:1206.6471*.

Shimodaira, Hidetoshi (2000). “Improving predictive inference under covariate shift by weighting the log-likelihood function”. In: *Journal of statistical planning and inference* 90.2, pp. 227–244.

Sugiyama, Masashi, Matthias Krauledat, and Klaus-Robert Müller (2007). “Covariate shift adaptation by importance weighted cross validation.” In: *Journal of Machine Learning Research* 8.5.

Sugiyama, Masashi, Taiji Suzuki, et al. (2008). “Direct importance estimation for covariate shift adaptation”. In: *Annals of the Institute of Statistical Mathematics* 60.4, pp. 699–746.

## A Proof of Lemma 2

Convex hulls of finite sets in  $\mathbb{R}^\ell$  are *convex* polytopes, which can be expressed as an intersection of  $h$  halfspaces indexed by  $f$  with  $\{\mathbf{x} : \mathbf{a}^{(f)\top} \mathbf{x} < b^{(f)}\}$  (Grünbaum et al., 1967). Vectors  $\mathbf{a}^{(f)\top}$  can be combined as row-vectors of a matrix,  $A$ , so that any convex polytope can be expressed as

$$\{\mathbf{x} : A\mathbf{x} < \mathbf{b}\} = \left\{ \mathbf{x} : \begin{pmatrix} (\mathbf{a}^{(1)})^\top \\ \vdots \\ (\mathbf{a}^{(h)})^\top \end{pmatrix} \mathbf{x} < \begin{pmatrix} b^{(1)} \\ \vdots \\ b^{(h)} \end{pmatrix} \right\}. \quad (12)$$

For convenience, the vectors  $\mathbf{a}^{(f)}, \tilde{\mathbf{a}}^{(f)}$  are assumed to be unit vectors throughout.

The idea behind the proof will be to analyze the movement of the boundaries of the polytope defined by  $\mathcal{V} = \{\mathbf{v}_1, \dots, \mathbf{v}_m\}$  and corresponding polytope defined by the “perturbed points”  $\tilde{\mathcal{V}} = \{\tilde{\mathbf{v}}_1, \dots, \tilde{\mathbf{v}}_m\}$ . The key is to show that a point that is far enough from the boundary of  $\text{Co}(\mathcal{V})$  will also be within  $\text{Co}(\tilde{\mathcal{V}})$ , given by Lemma 7. This required distance from the boundary will be relative to the amount by which the perturbed points have moved. As we bring the perturbation arbitrarily small (i.e.  $\varepsilon \rightarrow 0$ , all points in the interior of the polytope will be included).

**Lemma 7.** *Let*

$$\begin{aligned} \text{Co}(\mathcal{V}) &= \{\mathbf{x} : A\mathbf{x} < \mathbf{b}\} \\ \text{Co}(\tilde{\mathcal{V}}) &= \{\mathbf{x} : \tilde{A}\mathbf{x} < \tilde{\mathbf{b}}\} \end{aligned}$$

as given by Equation 12. If  $A\mathbf{x} < \mathbf{b} - \varepsilon\mathbf{1}_\ell$  and  $\|\mathbf{v}_i - \tilde{\mathbf{v}}_i\|_2 < \varepsilon \forall i$ , then  $\tilde{A}\mathbf{x} < \tilde{\mathbf{b}}$ .

To prove Lemma 7, we will need to show that the boundaries of the polytopes do not move too much. We will do this using Lemma 8, which bounds how far  $\text{Bo}(\text{Co}(\mathcal{V}))$  can be from  $\text{Bo}(\text{Co}(\tilde{\mathcal{V}}))$  along a single “face.”

**Definition 9.** Choose  $f \in [h]$ . Define:

$$\begin{aligned} W^{(f)} &= \{\mathbf{w} : (\mathbf{a}^{(f)})^\top \mathbf{w} = b^{(f)}, \mathbf{w} \in V\} \\ \tilde{W}^{(f)} &= \{\tilde{\mathbf{w}}_i : \mathbf{v}_i \in W^{(f)}\} \end{aligned}$$

We restrict the size of  $|W^{(f)}| = \ell$ , which is the number of points needed to define a halfspace in  $\mathbb{R}^\ell$ . This can be done by allowing for multiple identical  $\mathbf{a}_f, b_f$  combinations corresponding to all size  $\ell$  subsets of the  $v_i$  along the boundary.

Note that  $\text{Co}(W^{(f)})$  describes a “face” of the polytope  $\text{Co}(\mathcal{V})$  indexed by  $f$  which is perpendicular to  $\mathbf{a}^{(f)}$ .  $\text{Co}(\tilde{W}^{(f)})$  describes the perturbed face.

**Lemma 8.** *Choose  $f, g \in [h]$  arbitrarily and let  $W^{(f)} = \{\mathbf{w}_1^{(f)}, \dots, \mathbf{w}_\ell^{(f)}\}$  and  $\tilde{W}^{(f)} = \{\tilde{\mathbf{w}}_1^{(f)}, \dots, \tilde{\mathbf{w}}_\ell^{(f)}\}$ . For every  $\mathbf{m}^{(f)} \in \overline{\text{Co}}(W^{(f)})$ , we have  $(\tilde{\mathbf{a}}^{(g)})^\top \mathbf{m}^{(f)} < \tilde{b}^{(g)} + \varepsilon$ .*

*Proof.* Because  $m \in \overline{\text{Co}}(W^{(f)})$ , there is some  $\lambda \in \Delta_\ell$  with

$$\mathbf{m}^{(f)} = \sum_{i=1}^{\ell} \lambda_i \mathbf{w}_i^{(f)} \in \overline{\text{Co}}(W^{(f)}) \quad (13)$$

Consider also

$$\tilde{\mathbf{m}}^{(f)} = \sum_{i=1}^{\ell} \lambda_i \tilde{\mathbf{w}}_i^{(f)} \in \overline{\text{Co}}(\tilde{W}^{(f)}) \quad (14)$$

Note that the norm of the difference between these two vectors is bounded:

$$\begin{aligned} \|\mathbf{m}^{(f)} - \tilde{\mathbf{m}}^{(f)}\|_2 &= \left\| \sum_{i=1}^{\ell} \lambda_i (\mathbf{w}_i^{(f)} - \tilde{\mathbf{w}}_i^{(f)}) \right\|_2 \\ &\leq \sum_{i=1}^{\ell} \lambda_i \underbrace{\|\mathbf{w}_i^{(f)} - \tilde{\mathbf{w}}_i^{(f)}\|_2}_{< \varepsilon} < \varepsilon \end{aligned} \quad (15)$$

Also note that because  $\tilde{\mathbf{m}}^{(f)} \in \overline{\text{Co}}(\tilde{W}^{(f)}) \subseteq \overline{\text{Co}}(\tilde{V})$ , we have that  $(\tilde{\mathbf{a}}^{(g)})^\top \tilde{\mathbf{m}}^{(f)} \leq \tilde{b}^{(g)}$ . Now, a simple application of Cauchy-Schwartz gives:

$$\begin{aligned}
 (\tilde{\mathbf{a}}^{(g)})^\top \mathbf{m}^{(f)} &= (\tilde{\mathbf{a}}^{(g)})^\top (\tilde{\mathbf{m}}^{(f)} + (\mathbf{m}^{(f)} - \tilde{\mathbf{m}}^{(f)})) \\
 &= \underbrace{(\tilde{\mathbf{a}}^{(g)})^\top \tilde{\mathbf{m}}^{(f)}}_{\leq \tilde{b}^{(g)}} + (\tilde{\mathbf{a}}^{(g)})^\top (\mathbf{m}^{(f)} - \tilde{\mathbf{m}}^{(f)}) \\
 &\leq \tilde{b}^{(g)} + \left\| \tilde{\mathbf{a}}^{(g)} \right\|_2 \left\| \mathbf{m}^{(f)} - \tilde{\mathbf{m}}^{(f)} \right\|_2 \\
 &< \tilde{b}^{(g)} + \varepsilon
 \end{aligned} \tag{16}$$

□

With this, we are now ready to prove Lemma 7.

*Proof.* Choose an arbitrary face  $g \in [h]$ . Recall we have  $\mathbf{x} \in \text{Co}(V)$  with  $(\mathbf{a}^{(g)})^\top \mathbf{x} < b - \varepsilon$  and we wish to show  $(\tilde{\mathbf{a}}^{(g)})^\top \mathbf{x} < \tilde{b}^{(g)}$ .

Let  $\mathbf{m}_x^{(f)}$  be the result of extending  $\tilde{\mathbf{a}}^{(g)}$  from  $\mathbf{x}$  to  $\text{Bo}(V)$ . This must hit some face with  $(\mathbf{a}^{(f)})^\top \mathbf{m}_x^{(f)} = b^{(f)}$ , so  $\mathbf{m}_x^{(f)} \in \text{Co}(W^{(f)})$ . That is, find  $\beta$  such that

$$\mathbf{m}_x^{(f)} = \beta \tilde{\mathbf{a}}^{(g)} + \mathbf{x} \in \text{Co}(W^{(f)}) \tag{17}$$

First, lets bound  $\beta$ . Notice that because  $\mathbf{m}_x^{(f)} \in \text{Co}(W^{(f)})$ , we have

$$\begin{aligned}
 (\mathbf{a}^{(f)})^\top \mathbf{m}_x^{(f)} &= (\mathbf{a}^{(f)})^\top \left( \sum_{i=1}^{\ell} \lambda_i \mathbf{w}_i^{(f)} \right) \\
 &= \sum_{i=1}^{\ell} \lambda_i (\mathbf{a}^{(f)})^\top \mathbf{w}_i^{(f)} = b^{(f)}
 \end{aligned} \tag{18}$$

So, we have

$$b^{(f)} = (\mathbf{a}^{(f)})^\top \mathbf{m}_x^{(f)} = \underbrace{\beta (\mathbf{a}^{(f)})^\top \tilde{\mathbf{a}}^{(g)}}_{\leq 1} + \underbrace{(\mathbf{a}^{(f)})^\top \mathbf{x}}_{< b^{(f)} - \varepsilon} \Rightarrow \varepsilon < \beta \tag{19}$$

Now, apply Lemma 8

$$\begin{aligned}
 (\tilde{\mathbf{a}}^{(g)})^\top \mathbf{m}_x^{(f)} &< \tilde{b}^{(g)} + \varepsilon \\
 (\tilde{\mathbf{a}}^{(g)})^\top \mathbf{x} + (\tilde{\mathbf{a}}^{(g)})^\top \tilde{\mathbf{a}}^{(g)} \beta &< \tilde{b}^{(g)} + \varepsilon \\
 (\tilde{\mathbf{a}}^{(g)})^\top \mathbf{x} &< \tilde{b}^{(g)}.
 \end{aligned} \tag{20}$$

Face  $g \in [h]$  was chosen arbitrarily, so this holds for all halfspaces in the convex polytope. Hence, we have  $A\mathbf{x} \prec \mathbf{b}$ . □

## B Counts that Follow the Correct DAG

The paradox presented in Section 2 used counts yielding a distribution that does not precisely follow the given DAG. We will now show how to construct a similar set of counts with the statistics needed to imply the causal structure.

Consider the modified Table 3. The structure is copied from Table 2. If  $\alpha_1 = \alpha_2, \beta_1 = \beta_2$ , and  $\gamma_1 = \gamma_2$ , then we notice that the relative probabilities of  $\Pr(x)$  are given by the  $\alpha$ s,  $\beta$ s, and  $\gamma$ s. If these coefficients are all equal, then we have every row considered with equal weight, as in the main paper.

While setting all of the Greek coefficients to 1 provides a nice intuition for how the paradox emerges, it unfortunately does not give a distribution that obeys the requirements of the given DAG. In order for our distribution to (1) factorize according to the DAG and (2) be be faithful to the DAG, we must have the following properties:

1.  $T \not\perp\!\!\!\perp Y$
2.  $X \not\perp\!\!\!\perp Y$
3.  $T \not\perp\!\!\!\perp X$

$T$	$X$	Cancer	Virus	Allergies
$t^{(1)}$	$x^{(1)}$	$2\alpha_1$	$\alpha_1$	0
$t^{(1)}$	$x^{(2)}$	0	$2\beta_1$	$\beta_1$
$t^{(1)}$	$x^{(3)}$	$\gamma_1$	0	$2\gamma_1$
$t^{(0)}$	$x^{(1)}$	0	$\alpha_2$	$2\alpha_2$
$t^{(0)}$	$x^{(2)}$	$2\beta_2$	0	$\beta_2$
$t^{(0)}$	$x^{(3)}$	$\gamma_2$	$2\gamma_2$	0

 Table 3: A specification of counts for  $Y \in \{\text{Cancer, Virus, Allergies}\}$ .

4.  $T \not\perp\!\!\!\perp Y | X$
5.  $X \not\perp\!\!\!\perp Y | T$
6.  $T \not\perp\!\!\!\perp X | Y$

With all of the Greek coefficients set to 1, we notice that conditions 5,6 are met. The domain expertise setting effectively conditions on  $Y$  by restricting it's values. When restricted to two columns, we also meet condition 4.

The remaining conditions (as well as condition 4 in the broader case) can be met by varying the Greek coefficients. Attached code allows one to explore different settings to the Greek coefficients to achieve this paradox. One example is  $\alpha_1 = \beta_1 = \gamma_1 = 1$  and  $\alpha_2 = 1.1, \beta_2 = 1.2, \gamma_2 = 1.3$ .